

Chun-Chieh Wu* and Hsiu-Ju Cheng¹

* Department of Atmospheric Sciences, National Taiwan University

¹Central Weather Bureau, Taipei, Taiwan

1. INTRODUCTON

The evolution of the eyewall in tropical cyclones (TC) has always been an intriguing issue in TC thermodynamics and dynamics. The eyewall process also plays a very important role in affecting the intensity change of the TC. The paper documents an interesting eyewall evolution prior, during and after the landfall as a followup work of Wu et al. (2003). The satellite images (Fig. 1) show that interesting eyewall evolution processes occurred during the period when Typhoon Zeb (1998) devastated Luzon. The eyewall of Zeb shrank before landfall, and a wider eyewall reformed as Zeb left Luzon and reentered the ocean. The eyewall contracted again as it moved along the east coast of Taiwan. Similar features have also been observed in other storms, such as Typhoon Melor (2003) over Luzon and Hurricane Wilma (2005) over Yucatan, but they have never been documented and investigated in detail in the literature.

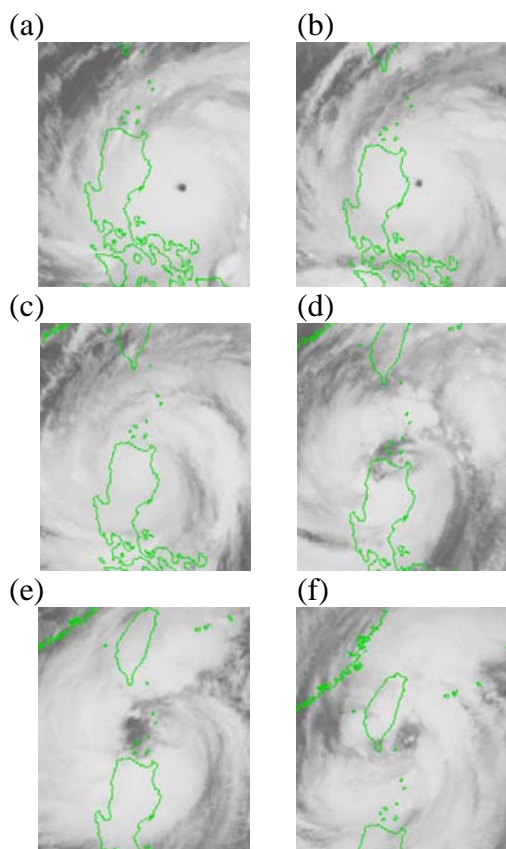


Fig. 1. GMS-5 infrared images of Typhoon Zeb(1998).

(a) 1800 UTC 13 Oct; (b) 0000 UTC 14 Oct; (c) 0600UTC 14Oct; (d) 1500UTC 14 Oct; (e) 0300 UTC 15 Oct; (f) 1500UTC 15 Oct.

The MM5 model with four nested domains (54/18/6/2-km resolution) was used to perform a 72-h simulation, starting from 0000 UTC 13 October 1998. The initial and lateral boundary conditions are based on the European Centre for Medium-range Weather Forecasts (ECMWF) Advanced global analysis. Three major numerical experiments with different underlying surface conditions are conducted to investigate the effect of the terrain of Luzon, its land surface, and the ocean on the eyewall evolution of Zeb. The control experiment (denoted as CTL) retains all the model-resolved terrain in the model domain. In the second simulation (denoted as NLT), the mountains of Luzon are flattened. In the third simulation (denoted as SEA), the land of Luzon is totally replaced by the ocean.

2. EYE AND EYEWALL EVOLUTION

Except for some slight northward deflection of the Zeb's track during the initial 24 h and an eastward bias after 48 h, the tracks of all the three experiments (Fig. 2) are in general agreement with the best track analysis of Zeb. The evolution of the minimum sea level pressure (MSLP) is also well simulated in CTL (Fig. 2), and NLT shows a similar MSLP tendency towards that in CTL. The comparable decreasing rates of MSLP in both NLT and CTL suggested that the weakening of Zeb after landfall is mainly associated with the cutoff of the lower surface heat fluxes.

The main features of eyewall contraction, breakdown, and reformation processes during the period when Zeb is near Luzon are well simulated in CTL. The contraction of the eyewall before landfall appears mainly associated with the increased low level convergence and upward motion as Zeb approached Luzon. The presence of the mountain terrain on Luzon plays some role in enhancing the above process. On the other hand, it is found that the breakdown and reformation of the eyewall after landfall are closely related to the effects of the different underlying surfaces. The low level equivalent potential temperature shows that the air under the eyewall cools and dries significantly after Zeb makes landfall. In CTL, the eyewall convection weakens significantly and the eyewall circulation dissipates gradually after Zeb makes landfall. The low level

* Corresponding author address: Chun-Chieh, Wu, Dept. of Atmospheric Sciences, National Taiwan University, No. 1, Sec. 4, Roosevelt Rd., Taipei, 106, Taiwan. E-mail: cwu@typhoon.as.ntu.edu.tw

maximum wind spins down while the radius of the maximum wind decreases. An outer eyewall forms in conjunction with the dissipation of the original inner eyewall. The formation of the outer eyewall is associated with the development and organization of the outer rain band. The larger eye appears as the outer eyewall intensifies and the inner eyewall disappears. Therefore, the radius of the eyewall after landfall does not change gradually, but jump abruptly from the smaller to the larger radius.

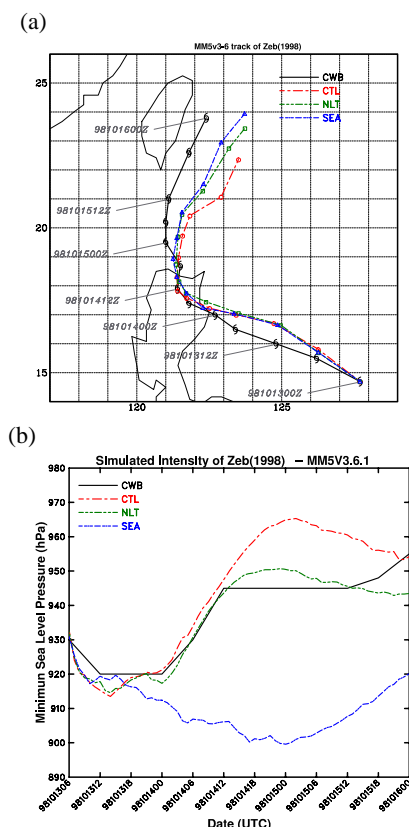


Fig. 2. (a) Best track of CWB and model tracks of all experiments; (b) Minimum sea level pressure of Typhoon Zeb.

The maximum surface heat flux inside Zeb's cyclonic circulation is found to be located underneath the eyewall when Zeb remains over the ocean. The surface heat flux under the eyewall decreases significantly when Zeb moves inland. Both the breakdown and reformation of the eyewall are associated with the availability of the surface heat flux from the lower boundary. From this point of view, the existence of Luzon plays the key role in the eyewall evolution in this case. The mountain plays an extra role in the weakening and dissipation of the original eyewall and the formation of the larger outer eyewall.

The evolution of the potential vorticity (PV) in CTL demonstrates different types of evolution when Zeb is located at land and over the sea. As shown in Figs. 3 and 4, the potential vorticity ring (Fig. 3a) evolves into a monopole (Fig. 3b) after Zeb makes

landfall. The low-level PV evolution (Figs. 3 and 4) after Zeb makes landfall bears some resemblance to the features of PV mixing between the eye and the eyewall described in Kossin and Eastin (2001) and Schubert et al. (1999), though in our case the PV mixing between the eye and the eyewall is enhanced by the increased friction after landfall. In other words, the surface friction exerts extra influence on the PV mixing while it weakens.

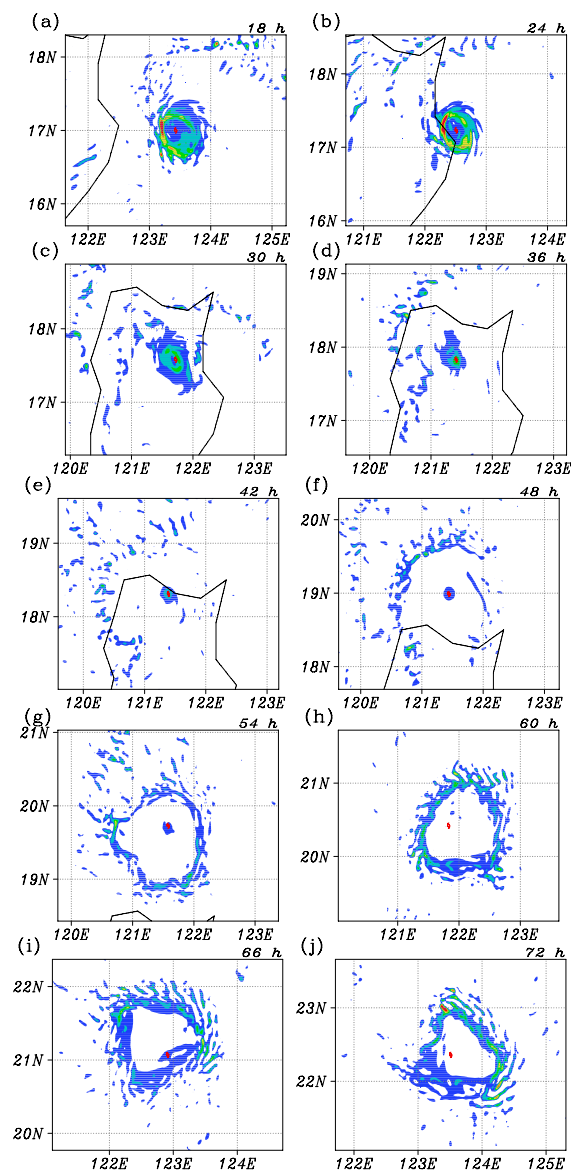


Fig. 3. The Potential vorticity at 875hPa in CTL. (a) 18h; (b) 24h; (c) 30h; (d) 36h; (e) 42h; (f) 48h; (g) 54h; (h) 60h; (i) 66h; (j) 72h.

When Zeb is about to reenter the ocean, the high PV ring associated with the new outer eyewall gradually forms (Figs. 3c, d), becomes well organized and persists until the end of the integration. While Zeb is moving northeastward toward the ocean southeast of Taiwan, the high PV ring of the new eyewall starts exhibiting some asymmetric wave-like structure. The very narrow high-PV-ring eyewall

continues to evolve into different asymmetric polygonal patterns with some mesoscale vortices in the eye. The PV budget analysis (details not shown) indicates that the diabatic heating contributes significantly to the production of high PV in the outer eyewall.

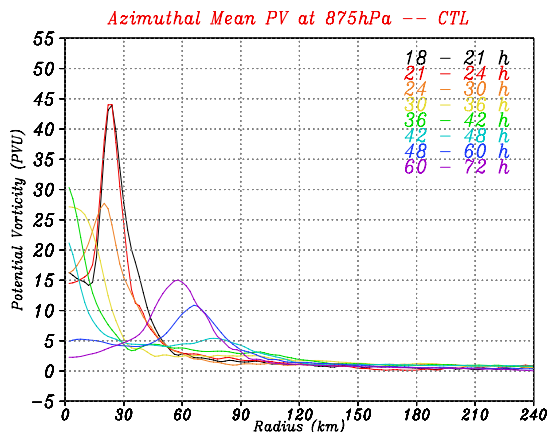


Fig. 4. The azimuthal mean Potential vorticity at 875hPa at different stages in CTL. (a)18h; (b)30h; (c)42h; (d)54h.

3. EVOLUTION OF THE OUTER EYEWALL RING

In our experiment, the evolution of PV in the eyewall is decisively influenced by the effects of surface friction and diabatic heating, suggesting that the moist convection is important to the evolution of the eyewall. Note that the dynamic evolution of the large eyewall ring has been studied by Kossin and Schubert (2001) based on the barotropic model, where they show that the ratio of the width of the vorticity ring to the radius of the ring at the initial state can lead to different end states with either vorticity crystals or monopole. To have a better understanding of the mechanism involved in the moist and frictional process affecting the evolution of the eyewall ring, several sensitivity experiments are conducted with or without moisture, PBL, or surface heat flux. Each of the new experiments starts with a PV ring with large radius, taken from the output of CTL at 54 h, and are integrated with the the boundary condition from the 54-72-h output of CTL. Each sensitivity run is integrated for 18 h on domain 4 (with 2-km horizontal resolution).

The sensitivity experiment (DFL) is integrated in the dry MM5 model without considering the planetary boundary layer (dry and frictionless, Fig. 5). The result shows that the high PV ring breaks down and dissipates (figures not shown). Integrated in the dry model with the planetary boundary layer (dry with friction), the sensitivity run (DRY) exhibits a more rapid weakening of the high PV ring. By the time the integration ends, the PV ring has broken up and dissipated. Unlike in CTL, DFL and DRY indicate that the eyewall ring cannot sustain itself when the diabatic

heating is turned off.

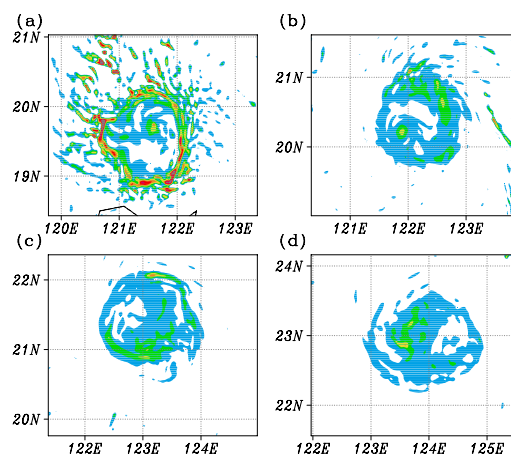


Fig. 5. Potential vorticity at $\sigma=0.875$ in DFL. (a) 0 h; (b) 6 h; (c) 12 h; (d) 18 h.

Another sensitivity experiment (NHF) is integrated into the moist MM5 model with the surface heat flux turned off. The high PV ring in NHF (Fig. 6) weakens and evolves rapidly into a monopole. On the other hand, the experiment (FL) with water yet without the planetary boundary layer in the model shows (figures not shown) a weakened and distorted PV ring at the end of the integration. The result presented above shows that the surface friction and the diabatic heating play quite important roles in the evolution of the typhoon eyewall. It is also found that the convective heating is strongly coupled with the vorticity field. In our sensitivity experiments, the more stable PV ring maintains in the presence of both the moist convection and the surface heat flux. The monopolar structure appears in the absence of the surface heat flux regardless of the presence of the friction.

During the eyewall evolution process, the surface friction acts to enhance the mixing between the eye and the eyewall while the diabatic heating enhances the PV in the eyewall. It is indicated that if the rate of PV production in the eyewall is more efficient than the rate at which the PV is advected or mixed away from the eyewall, the high PV ring can maintain and continue to intensify. In contrast to the result presented in Kossin and Schubert (2001), the very narrow high PV ring in our experiment maintains its ring-like structure until the end of simulation. The result of the above sensitivity experiment indicates the importance of the moist process and the property of the lower boundary in the evolution of the typhoon eyewall.

Our current result suggests that the influence of the heating is more than passive, and may possibly qualitatively change the behavior from purely advective dynamics. However, the detailed mechanism involved in the processes requires further

research through more specifically designed numerical experiments. It is expected that a suite of idealized model simulations with full physics could be used to gain more physical insights into the above interesting issues.

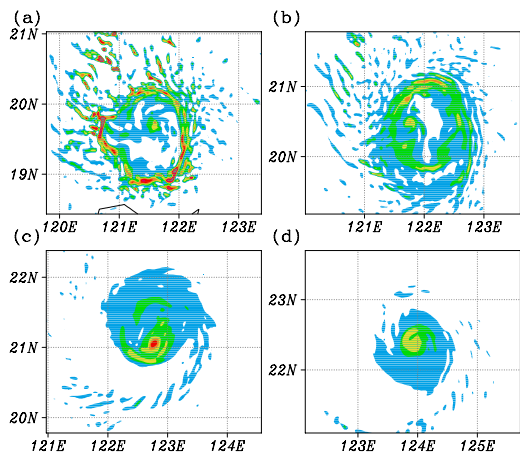


Fig. 6. Potential vorticity at $\sigma=0.875$ in NHF. (a) 0 h; (b) 6 h; (c) 12 h; (d) 18 h.

REFERENCES

- Kossin, J. P., and M. D. Eastin, 2001: Two Distinct regimes in the kinematic and thermodynamic structure of the hurricane eye and eyewall. *J. Atmos. Sci.*, **58**, 1079–1090.
- _____, and W. H. Schubert, 2001: Mesovortices, polygonal flow patterns, and rapid pressure falls in hurricane-like vortices. *J. Atmos. Sci.*, **58**, 2196–2209.
- Schubert, W. H., M. T. Montgomery, R. K. Taft, T. A. Guinn, S. R. Fulton, J. P. Kossin, and J. P. Edwards, 1999: Polygonal eyewalls, asymmetric eye contraction, and potential vorticity mixing in hurricanes. *J. Atmos. Sci.*, **56**, 1197–1223.
- Willoughby, H. E., and P. G. Black, 1996: Hurricane Andrew in Florida: Dynamics of a disaster. *Bull. Amer. Meteor. Soc.*, **77**, 543–549.
- Wu, C.-C., K.-H. Chou, H.-J. Cheng, and Y. Wang, 2003: Eyewall contraction, breakdown and reformation in a landfalling typhoon. *Geophys. Res. Lett.*, **30** (17), 1887, doi: 10.1029/2003GL01765.